

Stochastic Models of Implied Volatility Surfaces*

RAMA CONT[†] – JOSÉ DA FONSECA[‡] – VALDO DURRLEMAN[§]

We propose a market-based approach to the modelling of implied volatility, in which the implied volatility surface is directly used as the state variable to describe the joint evolution of market prices of options and their underlying asset. We model the evolution of an implied volatility surface by representing it as a randomly fluctuating surface driven by a finite number of orthogonal random factors. Our approach is based on a Karhunen–Loève decomposition of the daily variations of implied volatilities obtained from market data on SP500 and DAX options.

We illustrate how this approach extends and improves the accuracy of the well-known ‘sticky moneyness’ rule used by option traders for updating implied volatilities. Our approach gives a justification for the use of ‘Vegas’ for measuring volatility risk and provides a decomposition of volatility risk as a sum of independent contributions from empirically identifiable factors.

(J.E.L.: G130, C14, C31).

In the market for call/put options, option prices are often represented in term of the Black–Scholes implied volatilities, obtained by inverting the Black–Scholes formula given the market price of the option. It is empirically observed that the implied volatility $\Sigma_t(K, T)$ of a call option with exercise price K and maturity date T depends on (K, T) . The function

$$\Sigma_t : (K, T) \rightarrow \Sigma_t(K, T)$$

which represents this dependence is called the *implied volatility surface* at date t . It summarizes the state of the options market at data t .

Two features of this surface have captured the attention of researchers in

* We thank Andrea Berardi, Vincent Lacoste, Ole Barndorff Nielsen, Eric Reiner and seminar participants in Verona, HEC Montreal, Frontiers in Finance, RISK Math Week for their comments and suggestions.

[†] Centre de Mathématiques Appliquées, Ecole Polytechnique, F-91128 Palaiseau, France. E-mail: Rama.Cont@polytechnique.fr <http://www.cmap.polytechnique.fr/~rama/>

[‡] Ecole Supérieure d’Ingenierie Leonard de Vinci, F-91926 Paris La Defense, France. E-mail: jose.da_fonseca@devinci.fr

[§] Department of Operations Research and Financial Engineering, Princeton University, Princeton, NJ 08544.

financial modelling. First, the non-flat instantaneous profile of the surface, whether it be a ‘smile’, ‘skew’ or the existence of a term structure, point out to the insufficiency of the Black–Scholes model for matching a set of option prices at a given time instant and have led to various generalizations of the Black–Scholes model which aim at reproducing realistic instantaneous profiles for the surface $\Sigma_t(K, T)$. Second, the fact that the surface itself changes randomly with time as a result of supply and demand on the options market means that a good risk management model must not only fit the shape of $\Sigma_t(K, T)$ at a given date but also give realistic dynamics for $\Sigma_t(K, T)$ in time.

This paper presents a non-technical summary of our recent work on a market-based approach to the modelling of implied volatility, in which the implied volatility surface is directly used as the state variable to describe the joint evolution of market prices of options and their underlying asset. Our model is built on empirical facts and captures statistical properties of implied volatility dynamics in a parsimonious way.

We show how our stochastic implied volatility model allows a simple description of the time evolution of a set of options and provides a rationale for Vega hedging of portfolios of options. This modelling approach also allows us to construct a Monte-Carlo framework for simulating scenarios for the joint behaviour of a portfolio of call or put options, leading to a considerable gain in computation time for scenario generation.

The paper is structured as follows. Section 1 introduces the implied volatility surface and defines notations. Section 2 summarizes empirical findings on dynamics of implied volatility surfaces which are the foundation of our approach. Motivated by these facts, a factor model for implied volatility compatible with empirical observations is proposed in section 3. Some properties of the model are discussed in section 4. Evolution of call option prices is discussed in section 5. Section 6 discusses an application to Monte-Carlo simulation of a portfolio of options. Section 7 summarizes the results and discusses further applications.

1. Implied Volatility Surfaces

Recall that a European call option on a non-dividend paying asset S with maturity date T and strike price K is defined as a contingent claim with a pay-off of $(S_T - K)^+$. Denoting by $\tau = T - t$ the time remaining to maturity, the Black and Scholes (1973) formula for the value of this call option is

$$(1) \quad C_{BS}(S_t, K, \tau, \sigma) = S_t N(d_1) - Ke^{-r\tau} N(d_2)$$

$$\begin{aligned}
 d_1 &= \frac{-\ln m + \tau \left(r + \frac{\sigma^2}{2} \right)}{\sigma \sqrt{\tau}} \\
 d_2 &= \frac{-\ln m + \tau \left(r - \frac{\sigma^2}{2} \right)}{\sigma \sqrt{\tau}}
 \end{aligned}
 \tag{2}$$

where $m = K/S_t$ is the moneyness and

$$N(u) = (2\pi)^{-1/2} \int_{-\infty}^u \exp\left(-\frac{z^2}{2}\right) dz$$

Since the Black–Scholes price is strictly increasing with respect to the volatility, it defines a one-to-one map between prices and volatilities:

$$\forall y \in](S - Ke^{-r(T-t)})^+, S[, \exists! \sigma > 0, C_{BS}(S_t, K, \tau, \sigma) = y$$

Consider now, in a market where the hypotheses of the Black–Scholes model do not necessarily hold, a call option whose (observed) market price is denoted by $C_t^*(K, T)$. The Black–Scholes implied volatility $\Sigma_t(K, T)$ of the option is then defined as the value of the volatility parameter, which equates the market price with the price given by the Black–Scholes formula:

$$\exists! \Sigma_t(K, T) > 0, C_{BS}(S, K, \tau, \Sigma_t(K, T)) = C_t^*(K, T)$$

The Black–Scholes implied volatility thus defined is a widely used market indicator used by all options market practitioners and, as such, should be an object of interest for modelling the evolution of the options market.

From the implicit function theorem, one expects that, in general, Σ will depend on t, S, T, K (and, of course, on the randomness ω). For fixed (K, T) , $\Sigma_t(K, T)$ is, in general, a stochastic process and, for fixed t , its value depends on the characteristics of the option: the maturity T and the strike level K . The function $\Sigma_t : (K, T) \rightarrow \Sigma_t(K, T)$ is called the *implied volatility surface* at date t . Using the *moneyness* $m = K/S_t$ of the option, one can also represent the implied volatility surface as a function of moneyness and maturity:

$$I_t(m, \tau) = \Sigma_t(mS_t, t + \tau)$$

This representation is convenient because there is usually a range of moneyness around $m = 1$ for which the options are most liquid and, therefore, the empirical data are most readily available. The implied volatility surface today gives a snapshot of today’s market prices of vanilla options: given the current term structure of interest rates and dividends, specifying the implied volatility surface is equivalent to specifying prices of all vanilla options quoted on the market.

A large body of empirical and theoretical literature deals with the profile of the implied volatility surface for various markets as a function of (m, τ) (or

(K, T)) at a given date, i.e. with (t, S_t) fixed. While the Black–Scholes model predicts a flat profile for the implied volatility surface $I_t(m, \tau)$, it is a well-documented empirical fact that it exhibits both a non-flat strike and term structure (Das and Sundaram, 1999; Dumas *et al.*, 1998; Heynen, 1993; Rebonato, 1999). A typical illustration is given in Figure 1 in the case of DAX index options.

A plethora of models have been proposed to model the instantaneous profile in (m, τ) of the implied volatility surface: local volatility models, jump-diffusion models and stochastic volatility models with or without jumps.¹ These ‘smile’ models are defined in terms of stochastic differential equations whose parameters describe the *infinitesimal* evolution of the asset price: since this evolution is not directly observed, *calibration* of model parameters to market prices of options turns out to be an ill-posed problem whose numerical solution is not trivial. However, even in cases where perfect calibration to today’s option prices is achievable by a non-parametric model (for example, a local volatility model), a perfect fit of the implied volatility surfaces does not guarantee that the model will generate realistic future scenarios. This problem can be seen in the shape of the future smile (that is, the smile for forward-start options) generated by the model: many of these models, while giving good fits to today’s implied volatility/call prices generate unrealistic forms for future smiles, thus leading to a bias in prices of forward options.

As pointed out by Balland (2002), risk management of complex option positions requires not only a model that can calibrate today’s market implied volatilities but also a model which implies a realistic evolution of implied

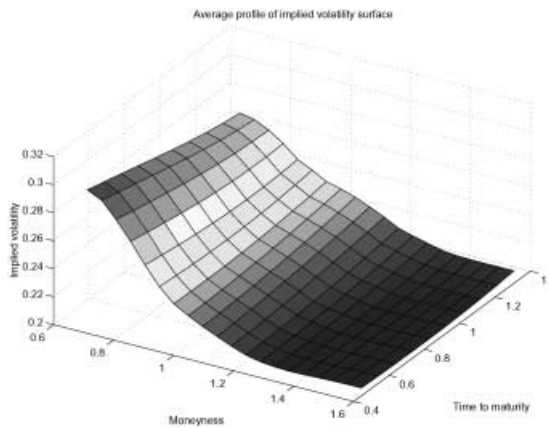


Figure 1: Average profile of the implied volatility of DAX options as a function of time to maturity and moneyyness, 1999–2001.

¹ See Avellaneda and Cont (2002) for recent reviews on these topics.

volatility. To achieve this, we must first study the statistical properties of implied volatility movements, reviewed in section 2.

2. Statistical Properties of Implied Volatility Surfaces

Empirical studies of the behaviour of implied volatilities of exchange-traded options on various market indices (SP500, FTSE, DAX and others) point to some statistical properties that seem to be common to these markets. These studies focus on three different aspects: profile across strikes (smile patterns), profile across maturities (term structure) and time series behaviour of implied volatilities. Each of these dependencies has been studied separately in different data sets: see Alexander (2001), Avellaneda and Zhu (1997), Das and Sundaram (1999), Heynen (1993), Heynen *et al.* (1994), Skiadopoulos *et al.* (2000), Fengler *et al.* (2000) and Hafner and Wallmeier (2001). Using a Karhunen–Loève decomposition of time series of volatility surfaces, Cont and Da Fonseca (2002) performed a joint study of dynamics of implied volatilities for all strikes and maturities for various index options. For more details and a survey of empirical studies we refer to Cont and Da Fonseca (2001, 2002) and references therein. We summarize here the main properties observed in implied volatility time series:

- 1 At a given date, the implied volatility surface has a non-flat profile and exhibits both strike and term structure.
- 2 The shape of the implied volatility surface undergoes deformation in time.
- 3 Implied volatilities display high (positive) autocorrelation and mean reverting behaviour.
- 4 The variance of the daily log-variations in implied volatility can be satisfactorily explained in terms of a small number of principal components (two or three).
- 5 The first principal component reflects an overall shift in the level of all implied volatilities.
- 6 The second principal component reflects opposite movements in (out of the money) call and put implied volatilities.
- 7 The third principal component reflects changes in the convexity of the surface.
- 8 Movements in implied volatility are not perfectly correlated with movements in the underlying asset.
- 9 Shifts in global level of implied volatilities are negatively correlated with the returns of the underlying asset.
- 10 Relative movements of implied volatilities have little correlation with the underlying.
- 11 The projections of the surface on its principal components ('principal component processes') exhibit high (positive) autocorrelation and mean reversion over a time-scale close to a month.

12 The autocorrelation structure of principal component processes is well approximated by AR(1)/Ornstein–Uhlenbeck process.

See Cont and Da Fonseca (2001, 2002) and references therein for more details.

3. A Model for the Joint Evolution of the Underlying and the Implied Volatility Surface

Based on these observations, we propose a model for joint evolution of an asset $S(t)$ and the implied volatility surface associated to options written on this asset. Section 3.1 describes the stochastic evolution of the implied volatilities. Section 3.2 then describes the dynamics of the underlying asset.

3.1. A Factor Model for the Implied Volatility Surface

Based on these empirical results, we have proposed (Cont and Da Fonseca 2002) a flexible class of models which is compatible with these observations. The state variables are (I_t, S_t) where S_t is the underlying asset and

$$(6) \quad I_t : [m_{\min}, m_{\max}] \times [\tau_{\min}, \tau_{\max}] \rightarrow [0, \infty[$$

is a smooth surface representing the implied volatility surface at date t . The implied volatility surface I_t is modelled as a stationary random surface evolving in a low dimensional manifold of surfaces.

More precisely, following Cont and Da Fonseca (2002), the (log-)implied volatility surface $X_t(m, \tau) = \ln I_t(m, \tau)$ is represented by its components on an orthonormal basis $(f_k, k = 1 \dots d)$:

$$(7) \quad \ln I_t(m, \tau) = X_t(m, \tau) = X_\infty(m, \tau) + \sum_{k=1}^d x_k(t) f_k(m, \tau)$$

$$x_k(t) = \langle X_t, f_k \rangle$$

$$(8) \quad \langle f_j, f_k \rangle = \iint f_j(m, \tau) f_k(m, \tau) dm d\tau = \delta_{j,k}$$

where the components x_k are Ornstein–Uhlenbeck processes driven by independent noise sources Z_k , which can be Wiener or jump processes:

$$(9) \quad X_t(m, \tau) = \sum_{k=1}^d x_k(t) f_k(m, \tau)$$

$$(10) \quad dx_k(t) = -\lambda_k(x_k(t) - \bar{x}_k)dt + \gamma_k dZ_k(t) \quad k = 1 \dots d$$

Here λ_k represents the speed of mean reversion of along the k th eigenmode

and γ_k is the volatility of implied vols along this direction. In empirical data, λ_k^{-1} is found to be close to a month (Cont and Da Fonseca, 2002).

Typically, we can take $d \leq 3$, $d = 2$ already gives a good approximation to the observed deformations of the surface over several months. For the principal directions of deformation of the surface, one may estimate them directly from the data by principal component analysis (Cont and Da Fonseca, 2002): empirical examples are shown in Figures 2, 3 and 4. Alternatively, one may use ‘stylized’ versions to represent f_1 as a level effect, f_2 as a slope effect and f_3 as a change in curvature:

$$(11) \quad f_1(m, \tau) = a_1$$

$$(12) \quad f_2(m, \tau) = a_2(\tau)m + b_2$$

$$(13) \quad f_3(m, \tau) = a_3m^2 + b_3m + c_3$$

The coefficients may be chosen to have a dependence in τ so as to reproduce the term structure of implied volatility. For example, one may choose

$$a_2 = A_2 \exp(-\gamma_2\tau)$$

to represent the decay of the skew with time to maturity as in Rebonato (1999).

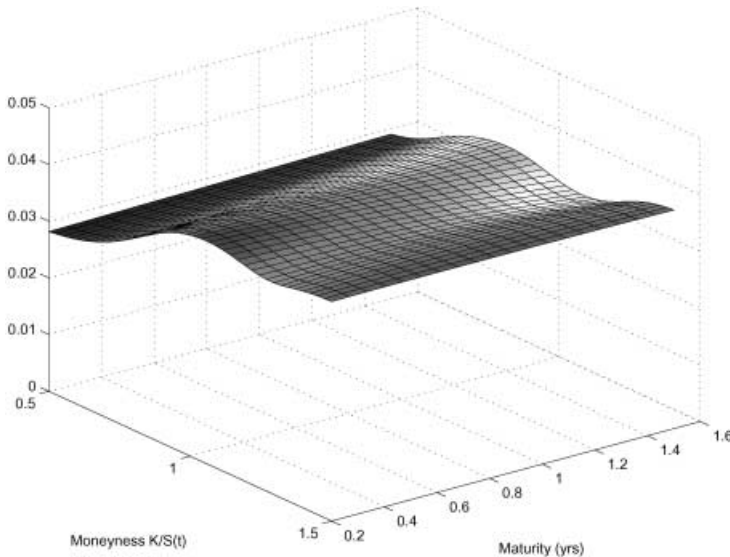


Figure 2: First principal component f_1 of daily implied volatility variations for SP500 index options. Shocks along this direction, which account for around 80 per cent of the daily variance of implied volatilities, can be interpreted as a level effect.

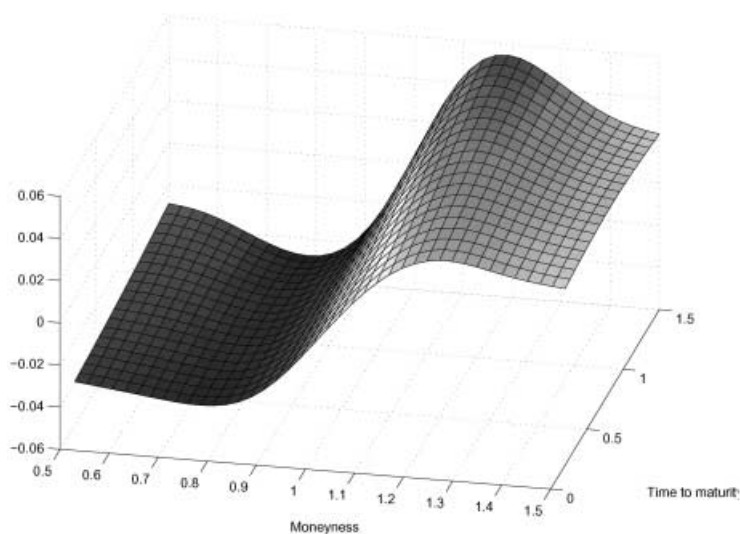


Figure 3: Second principal component f_2 of daily implied volatility variations for SP500 index options.

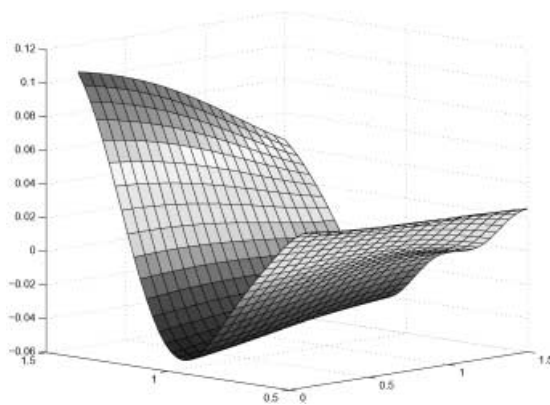


Figure 4: Third principal component f_3 of daily implied volatility variations for SP500 index options.

3.2. Evolution of the Underlying Asset

To compute dynamics of option prices, one needs to specify the dynamics of the underlying asset. One possibility is to describe the

$$(14) \quad \frac{dS_t}{S_t} = \mu dt + \alpha_0(t)dZ_t^0 + \sum_{k=1}^d \alpha_k(t)dZ_k(t)$$

where Z^k are independent noise terms and Z^0 represents the idiosyncratic risk in the underlying asset which is uncorrelated with the options market. For example, Z^k , $k = 0 \dots d$ can be independent Wiener processes.

$\alpha_0(t) \neq 0$ leads to an imperfect correlation between the underlying asset and the implied volatility surface. Empirical results indicate a strong negative correlation between movements in the level of implied volatility and the underlying returns. This can be captured by imposing $\alpha_1(t) < 0$. The magnitude of α_i , $i > 2$ is expected to be small (Cont and Da Fonseca, 2002).

Let us discuss now the relation between the two processes. Let \mathcal{F}_t^S , \mathcal{F}_t^I be respectively the filtrations generated by (S_t) and $I_t(m, \tau)$. In a one-factor complete market model, such as a local volatility model, the option prices can be attained by dynamic hedging strategies involving the underlying asset only, so the information contained in the option prices is redundant with respect to the information in \mathcal{F}_t^S : $I_t(m, \tau)$ is an \mathcal{F}_t^S -adapted process.

In the model presented above, this is not the case: in general, neither \mathcal{F}_t^I is contained in \mathcal{F}_t^S , nor the other way round. This is an important property of the model and corresponds indeed to the real situation encountered on the market: option prices can be affected by factors other than the underlying asset; and, inversely, although market prices of options do give some information on the underlying asset, there is not enough information on the options market to retrieve, in a unique way, the implied dynamics of the underlying asset. This is, by the way, the fundamental reason the problem of calibrating smile models to option prices is ill-posed in general.

Arbitrage restrictions on stochastic models for implied volatilities were considered in Schönbucher (1999), Brace *et al.* (2001) and Ledoit and Santa Clara (1999) in a risk neutral framework. Note that here we have to consider, from a risk management perspective, the real dynamics of the implied volatilities and not the risk neutral dynamics, which may be very different. For example, it is shown in Schönbucher (1999) that, in a model with a single implied volatility, the risk neutral implied volatility has a mean-fleeing (opposite of mean reverting!) behaviour. The relation between risk neutral and historical dynamics is discussed in more detail in Cont and Durrleman (2002).

3.3. Nature of Noise Terms

As observed in Cont and Da Fonseca (2002), while it may appear more convenient to choose Wiener processes as noise sources, this is not necessarily the best choice. First, from an empirical point of view, the movements in implied volatility can exhibit jumps: in the case of FTSE implied volatilities, the second principal component process is observed to have heavy-tailed increments with jump-like movements (Cont and Da Fonseca, 2002, figs 22 and 23). This observation pleads for the inclusion of jump terms in the evolution of I_t (in this case, in Z^2). Second, as shown by Balland (2002), in the

limiting case where the implied volatility surface $I_t(m, \tau)$ is a non-flat surface constant in time, i.e. $I_t(m, \tau) = I_0(m, \tau)$, the *risk neutral* dynamics of the underlying asset is a jump process with independent increments. Although a typical sample path may be very different under the historical dynamics which we model here, the trajectories of the price will remain discontinuous in both cases. This observation pleads for including a jump term in the evolution of S_t otherwise the ‘fixed smile’ case cannot be included.

4. Properties

Now let us outline some of the properties of the proposed stochastic model.

- 1 The implied volatilities have a random behaviour in time, but have a smooth dependence in (K, T) .
- 2 Implied volatilities $I_t(m, \tau)$ and $\Sigma_t(K, T)$ are positive. In the case where the noise terms are taken to be Wiener processes, $I_t(m, \tau)$, is, in fact, a log normal random variable.
- 3 Implied volatility $I_t(m, \tau)$ is mean reverting with a mean reversion time that is empirically found to be around one or two months. This means that, for short maturity options (with maturity less than one month for example), the implied volatility surface will not move away too much from its current position. Therefore, ‘forward smiles’ will be similar to the current smile if one is interested in looking a month or so ahead of the current time. For forward-start options starting in several months (which is long compared to the mean reversion time), $I_t(m, \tau)$ will approximately behave according to the invariant measure of (9) so it will resemble the typical long-term average of its profile. Figure 1 shows the profile of such an average smile (here, averaged over a sample of 2 years, 1999–2001). One can readily observe that the skew is not flattened, contrarily to the problem encountered for forward smiles in local volatility models. In particular, in the stationary case (where $I_t(m, \tau)$ is a stationary random surface) 3-month implied volatilities will have the same distribution at any starting date in the future, so the 3-month forward smile will be a stationary random curve i.e. its statistical properties will not depend on the starting time of the option.
- 4 Calibration to market implied volatilities is simply reduced to specifying the initial condition: $x_0(m, \tau) = \ln I_0(m, \tau)$: any market smile/term structure can be exactly incorporated into the model.
- 5 The model allows easy evaluation of any portfolio of vanilla options: the price of any call option $C_t(T, K)$ is simply given by the Black–Scholes formula:

$$\begin{aligned}
 C_t(K, T) &= C_{BS}(S_t, K, \tau, \Sigma_t(K, T)) \\
 (15) \qquad &= C_{BS}\left(S_t, K, \tau, I_t\left(\frac{K}{S_t}, T - t\right)\right)
 \end{aligned}$$

This is obviously true at the current date but also at any future date in any scenario generated in a Monte-Carlo simulation of the factor model. In particular, it suggests a simple way of generating joint scenarios for implied volatilities (see section 6). This property should be contrasted for example with the approach of Derman and Kani (1998) where the *local* volatility surface is modelled as a random surface: in that case, the impact on option prices is complicated and requires solving a PDE.

5. Evolution of European Call Options

As mentioned above, the price of a European call (or put) option is simply given by applying the Black–Scholes formula to the current implied volatility surface. The dynamic evolution of a call option is therefore given by Ito’s formula:

$$\begin{aligned}
 dC_t(K, T) &= \frac{\partial C_{BS}}{\partial t} dt + \frac{\partial C_{BS}}{\partial S} dS_t + \frac{\partial C_{BS}}{\partial \Sigma} d\Sigma_t(K, T) \\
 &\quad + \frac{1}{2} \frac{\partial^2 C_{BS}}{\partial S^2} d\langle S \rangle_t + \frac{1}{2} \frac{\partial^2 C_{BS}}{\partial \Sigma^2} d\langle \Sigma_t(K, T) \rangle \\
 &\quad + \frac{\partial^2 C_{BS}}{\partial \Sigma \partial S} d\langle \Sigma_t(K, T), S \rangle_t \\
 (16) \qquad &= \theta_t dt + \Delta_t dS_t + \text{Vega} d\Sigma_t(K, T)
 \end{aligned}$$

where $\Sigma(K, T)$ is the implied volatility for a given strike K and maturity date T . One therefore requires the evolution of the fixed-strike volatility $\Sigma(K, T)$, the quadratic variations of the fixed-strike volatility, the quadratic variation of S and their joint variation.

Proposition 1 *Evolution of fixed strike implied volatilities* The fixed-strike implied volatility $\Sigma(K, T)$ follows the dynamics

$$\frac{d\Sigma_t(K, T)}{\Sigma_t(K, T)} = \frac{\alpha^2(t)}{2} \left(\sum_{k=1}^d x_k(t) \frac{K}{S_t} \partial_{mf_k} \right)^2$$

$$\begin{aligned}
 & + \sum_{k=1}^d \left[\lambda_k \bar{x}_k f_k + \frac{\gamma_k^2}{2} f_k^2 + \frac{\gamma_k K \alpha_k(t)}{S_t} \partial_m f_k \right. \\
 & \left. + x_k(t) \left(\partial_m f_k \frac{K(\alpha_t^2 - \mu - \sum_{j=1}^d \gamma_j \alpha_j(t) f_j)}{S_t} + \frac{K^2 \alpha_t^2 \partial_m^2 f_k}{2S_t} - \lambda_k f_k - \partial_\tau f_k \right) \right] dt \\
 & + \sum_{k=1}^d \left[\gamma_k f_k - \frac{K \alpha_j(t)}{S_t} \left(\sum_{j=1}^d x_j(t) \partial_m f_j \right) \right] dW_j(t)
 \end{aligned}
 \tag{17}$$

Given the stochastic equation governing a fixed-strike implied volatility, it is now straightforward to derive the evolution of a European call option by substituting (17) in (16):

Proposition 2 *Evolution of European call option* The price of a European call option $C_t(T, K)$ follows the dynamics

$$\begin{aligned}
 dC_t(T, K) &= M_t dt + s_t \sum_{j=0}^d \left[N(d_1) \alpha_j(t) \right. \\
 & \left. + n(d_1) \Sigma_t(K, T) \sqrt{T-t} \left(\gamma_j f_j - \alpha_j(t) \sum_{k=1}^d x_k(t) \frac{K}{S_t} \partial_m f_k \right) \right] dW_t^j \\
 &= M_t dt + S_t \Delta_t(T, K) \sum_{j=0}^d \alpha_j(t) dW_t^j \\
 & + \text{Vega}_t(T, K) \sum_{j=0}^d \left[\gamma_j f_j - \alpha_j(t) \sum_{k=1}^d x_k(t) \frac{K}{S_t} \partial_m f_k \right] dW_t^j
 \end{aligned}
 \tag{18}$$

where M_t is a drift term; see Cont and Durrleman (2002) for details. The random terms are thus decomposed into a sum of two terms:

- a term proportional to the Black–Scholes delta of the option, already present in a local volatility model
- a term proportional to the Black–Scholes vega, representing the volatility risk of the option.

Note that the sensitivities appearing in (18) are the usual Black–Scholes sensitivities and are not model dependent, showing that the usual Black–Scholes vegas will be the relevant sensitivities to compute in this modelling approach.

This evolution equation is verified by the call option price $C_t(K, T)$ up to a stopping time

$$(19) \quad \theta = \inf\{T - \tau_{\min}, \theta_0\}$$

$$(20) \quad \theta_0 = \inf\left\{t \geq 0, \frac{K}{S_t} \notin [m_{\min}, m_{\max}]\right\}$$

This makes sense since at the stopping time θ

- either the option has moved too far from the money and the impact of implied volatility on its time value is negligible, or
- the option is too close to maturity (a few days typically) and again its time value is close to zero.

In both cases, the information given by the implied volatility is irrelevant for pricing the option and the behaviour of the option is not governed any more by its implied volatility but by its intrinsic value.

The continuous time equation (18) is not useful for numerical simulation for which one should of course use the integrated form (15). However, (18) can be used to compute a Delta-Vega hedge: the delta and vega of any position in vanilla options can be offset in this model by a portfolio consisting in the underlying asset and d liquid vanilla options. The situation is similar to the one in fixed income markets where, in a d -factor interest rate model, any fixed income position can be hedged with d bonds plus the numeraire.

6. Monte-Carlo Simulation of Portfolios of Options

A common way of measuring the risk of a complex market position in vanilla options is to examine the profit and loss (P&L) of the portfolio in various plausible market scenarios and quantify the risk of the position by a measure of dispersion on the P&L distribution such as a moment, a quantile (VaR) or any other indicator. A systematic computational approach used in this context is a Monte-Carlo simulation: one starts by generating N scenarios ω_i , $i = 1, \dots, N$ for the underlying asset(s) using a stochastic model \mathcal{M} ; then one evaluates the portfolio's P&L in each scenario at some given time horizon t .

To evaluate the portfolio in each scenario, one must be able to price each option in each scenario. This can either be done using a model which is sufficiently tractable to provide a 'closed' form pricing formula: examples are the Black-Scholes model, an affine model such as the Heston stochastic volatility model or affine jump-diffusion models. One can then compute the value of options at time t in scenario ω_i using as input the current value of the underlying $S_t(\omega_i)$. Unfortunately, such models are unable to capture/calibrate the initial profile of the market implied volatility surfaces (especially the term structure of the implied volatilities (Das and Sundaram, 1999; Gatheral, 2001;

Busca and Cont, 2002; Tompkins, 2001), so one cannot incorporate the information on the initial smiles into them.

An alternative approach is then to use a model for the underlying asset which is capable of fitting the initial volatility surface. This is the case for example if one uses a non-parametric local volatility model (Dupire model):

$$(21) \quad \frac{dS_t}{S_t} = \mu dt + \sigma(t, S_t) dW_t$$

where the local volatility surface $\sigma(\cdot, \cdot)$ is calibrated to match the initial implied volatility surface $I_0(\cdot, \cdot)$. Prices of call options are not given in closed form but may be computed for all future dates and scenarios by solving numerically the generalized Black–Scholes partial differential equation:

$$(22) \quad \frac{\partial C}{\partial t} + rx \frac{\partial C}{\partial x} + \frac{x^2 \sigma^2(t, x)}{2} \frac{\partial^2 C}{\partial x^2} - rC(t, x; T, K) = 0$$

$$(23) \quad \forall x \geq 0 \quad C(T, x; T, K) = (x - K)^+$$

A known problem with this approach is that, when the calibration is done at $t = 0$ and the model is translated forward in time, it produces a future smile pattern that flattens out: the ‘forward smile’ cannot be time invariant (Bereystycki *et al.*, 2002). This is related to the fact that the local volatility surface is parametrized by absolute maturity T (as opposed to relative maturity τ).

Our mean reverting model for the implied volatility surface provides a simple approach to the simulation of scenarios for the joint evolution of a portfolio of call and put options which avoids these problems.

First, since the initial condition I_0 is chosen to be the current market surface, there is no issue with calibration so the model can take into account the current volatility smile. Second, as noted in section 4, the implied volatilities for forward-start options behave in a similar way to those today: in the special case of the stationary model, in fact, the model becomes time invariant. In particular, the forward smile does not flatten out: it will fluctuate around its long-term average.

Moreover, since the parameters are estimated to match the statistical properties of the time evolution of implied volatilities, the scenarios generated for future smiles will be similar to those seen in historical data and coherent with the type of evolution seen in the market.

A popular approach for marking to market exotic option deals is to use static or quasi static replication (Carr *et al.*, 1998; Allen and Padovani, 2002): this technique reduces an exotic position to a portfolio of vanilla calls and puts. In this case, such a portfolio can be readily priced in a Monte-Carlo sample path using the same approach as above.

Such approaches have already been considered in the case where the at-the-money implied vol is perturbed by random shocks while the shape of the smile is fixed: Malz (2001) uses this approach for stress-testing; see also

Rosenberg (2000). Our framework allows an extension to the case of a random smile/surface. A similar approach is proposed by Härdle and Schmidt (2000).

7. Conclusion

We have outlined a modelling approach based on using the implied volatility surface as a stochastic state variable representing the dynamics of the option market. After describing the empirical aspects such a model should incorporate, we have given a family of models which exhibit these properties. The basic framework is that of a linear factor model for the log of implied volatilities with mean reverting Ornstein–Uhlenbeck processes used as factors. The structure of the model allows for easy estimation of the parameters from historical data.

In addition to simplicity, the random surface model possesses two interesting features: first, any initial smile and term structure of implied volatilities can be input into the model; and second, it generates a realistic future evolution for the implied volatility surface in contrast with local volatility or stochastic volatility models.

These models allow a simple approach for quantifying and hedging of volatility risk, defined in terms familiar to practitioners in the options market. We suggest, in particular, an application to Monte-Carlo simulation of option portfolios for computing volatility risk exposures.

Another field in which this approach has potentially interesting applications is the hedging and risk management of ‘volatility derivatives’ such as volatility swaps or options on implied volatility.

These issues shall be addressed in a forthcoming work.

REFERENCES

- C. ALEXANDER (2001), "Principles of the Skew", *RISK*, January, S29–32.
- S. ALLEN - O. PADOVANI (2002), "Risk Management using Quasi Static Hedging", *Economic Notes*, this issue.
- M. AVELLANEDA - R. CONT (eds) (2002), Special Issue on Volatility modeling, *Quantitative Finance*, 2(1).
- M. AVELLANEDA - Y. ZHU (1997), "An E-ARCH Model for the Term Structure of Implied Volatility of FX Options", *Applied Mathematical Finance*, 4, pp. 81–100.
- P. BALLAND (2002), "Deterministic Implied Volatility Models", *Quantitative Finance*, 2(1).
- H. BERESTYCKI - J. BUSCA - I. FLORENT (2002), "Asymptotics and Calibration of Local Volatility Models", *Quantitative Finance*, 2(1), pp. 61–70.
- F. BLACK - M. SCHOLES (1973), "The Pricing of Options and Corporate Liabilities", *Journal of Political Economy*, 81, pp. 637–54.
- A. BRACE - B. GOLDYS - F. KLEBANER - R. WOMERSLEY (2001), "Market Model of Stochastic Implied Volatility with Application to the BGM Model", Working paper S01-1, Department of Statistics, University of New South Wales.
- J. BUSCA - R. CONT (2002), "Properties of Option Prices in Exponential Lévy Models", Working Paper, CMAP, Ecole Polytechnique.
- P. CARR - P. ELLIS - V. GUPTA (1998), "Static Hedging of Exotic Options", *Journal of Finance*, LIII(3), pp. 1161–90.
- R. CONT - J. DA FONSECA (2001), "Deformation of Implied Volatility Surfaces: An Empirical Study", in H. Takayasu (ed.), *Empirical Science of Financial Fluctuations*, Springer, Tokyo, pp. 230–9.
- R. CONT - J. DA FONSECA (2002), "Dynamics of Implied Volatility Surfaces", *Quantitative Finance*, 2(1), pp. 45–60.
- R. CONT - V. DURRLEMAN (2002), in preparation.
- S. R. DAS - R. K. SUNDARAM (1999), "Of Smiles and Smirks: A Term Structure Perspective", *Journal of Financial and Quantitative Analysis*, 34(2), pp. 211–40.
- E. DERMAN - I. KANI (1998), "Stochastic Implied Trees: Arbitrage Pricing with Stochastic Strike and Term Structure", *International Journal of Theoretical and Applied Finance*, 1, pp. 61–110.
- B. DUMAS - J. FLEMING - R. E. WHALEY (1998), "Implied Volatility Functions: Empirical Tests", *The Journal of Finance*, 8(6), pp. 2059–106.
- M. FENGLER - W. HÄRDLE - C. VILLA (2000), "The Dynamics of Implied Volatilities: A Common Principal Component Approach", Working paper, Humboldt Universität, Berlin.

- J. GATHERAL (2001), "Fitting the Implied Volatility Skew", (lecture notes), NYU Courant Institute.
- R. HAFNER - M. WALLMEIER (2001), "The Dynamics of DAX Implied Volatilities", *Quarterly International Journal of Finance*, 1, S1–27.
- W. HÄRDLE - P. SCHMIDT (2000), "Common Factors Governing VDAX Movements and the Maximum Loss", Humboldt University Working paper.
- R. HEYNEN (1993), "An Empirical Investigation of Observed Smile Patterns", *Review of Future Markets*, 13, pp. 317–53.
- R. HEYNEN - A. KEMMA - T. VORST (1994), "Analysis of the Term Structure of Implied Volatilities", *Journal of Financial and Quantitative Analysis*, 29(1), pp. 31–56.
- O. LEDOIT - P. SANTA CLARA (1999), "Relative Pricing of Options with Stochastic Volatility", UCLA Working paper.
- A. MALZ (2001), "Do Implied Volatilities Provide an Early Warning of Market Stress?", *Journal of Risk*, 3(2).
- R. REBONATO (1999), *Volatility and Correlation in the Pricing of Equity, FX and Interest Rate Options*, Wiley, New York.
- J. V. ROSENBERG (2000), "Implied Volatility Functions: A Reprise", *Journal of Derivatives*, 7(3).
- P. J. SCHÖNBUCHER (1999), "A Market Model for Stochastic Implied Volatility", *Philosophical Transactions of Royal Society, Series A*, 357(1758), August, pp. 2071–92.
- G. SKIADOPOULOS - S. HODGES - L. CLELOW (2000), "Dynamics of the S&P500 Implied Volatility Surface", *Review of Derivatives Research*, 3(3), pp. 263–82.
- R. TOMPKINS (2001), "Stock Index Futures Markets: Stochastic Volatility Models and Smiles", *The Journal of Futures Markets*, 21(1), pp. 43–78.